

PACS: 71.15.Mb; 71.20.-b; 71.55.Ak

## DUCTILE AND METALLIC NATURE OF $\text{Co}_2\text{VZ}$ ( $Z = \text{Pb, Si, Sn}$ ) HEUSLER COMPOUNDS: A FIRST PRINCIPLES STUDY

 Sukhender<sup>a</sup>,  Pravesh Pravesh<sup>b</sup>,  Lalit Mohan<sup>a</sup>,  Ajay Singh Verma<sup>\*a</sup>

<sup>a</sup>Department of Physics, Banasthali Vidyapith, Banasthali 304022, India

<sup>b</sup>Department of Electronics and Communication Engineering, KIET Group of Institutions Ghaziabad, Uttar Pradesh (India) 201206

\*Corresponding Author: [ajay\\_phy@rediffmail.com](mailto:ajay_phy@rediffmail.com)

Received April 21, 2020; accepted May 25, 2020

Herein, optoelectronic, elastic and magnetic properties of  $L_{21}$  structured  $\text{Co}_2\text{VZ}$  ( $Z = \text{Pb, Si, Sn}$ ) full Heusler compounds have been investigated by two methods. One is full potential linearized augmented plane wave (FP-LAPW) method as implemented in WIEN2k and second is pseudo potential method as implemented in Atomistic Tool Kit-Virtual NanoLab (ATK-VNL). All these compounds shows zero band gap in majority spin channel in the both simulation codes and a finite band gap are 0.33 and 0.54 eV in  $\text{Co}_2\text{VZ}$  ( $Z = \text{Pb, Sn}$ ) alloys (semiconducting) respectively. This is due to minority-spin channel near the Fermi level as implemented in WIEN2k code and showing 100% spin polarization except  $\text{Co}_2\text{VSi}$  (metallic) with zero band gap. These compounds found to be perfectly half-metallic ferromagnetic (HMF). However, above mentioned compounds shows finite band gaps in ATK-VNL code. The calculated magnetic moment of these compounds  $\text{Co}_2\text{VZ}$  ( $Z = \text{Pb, Si, Sn}$ ) are 3.00 and 3.00, 3.02 and 2.96, 3.00 and  $3.00\mu_B$  in WIEN2k and ATK-VNL codes respectively. Thus, we have observed that the calculated values by these simulation codes and Slater-Pauling rule have nice tuning. Optical properties of these compounds like as reflectivity, refractive index, excitation coefficient, absorption coefficient, optical conductivity and electron energy loss have been analyzed. Absorption coefficient and electron energy - loss function values are increases as we increase the value of energy. The values of Pugh's ratio  $B/G$  is greater than 1.75 for all compounds and showing ductile nature with positive value of Cauchy pressure ( $C_P = C_{12} - C_{44}$ ) and shows metallic behavior of  $\text{Co}_2\text{VZ}$  ( $Z = \text{Pb, Si, Sn}$ ) compounds.

**KEYWORDS:** Half-metallic ferromagnetic, band gap, Spintronics, magnetic moment, elastic constants

Half metallic ferromagnetic behavior of Heusler alloys fascinates the new researchers towards it, because exclusive approach in Spintronics [1-3]. If either one spin channel shows band gap and other shows zero band gap at Fermi level then the Heusler compounds exhibit 100% spin polarization [4-7]. Half metallic ferromagnetic was first discovered by de Groot in the year of 1983 in a half Heusler compound  $\text{NiMnSb}$  [8-9]. Due to high Curie temperature and spin magnetic moment, researchers show intensive interest in Heusler [10-11]. We are here going to investigate the properties of Co-based full Heusler compounds  $\text{Co}_2\text{VZ}$  ( $Z = \text{Pb, Si, Sn}$ ). Half metallic ferromagnetism in Co-based full Heusler compounds  $\text{Co}_2\text{MnSn}$ ,  $\text{Co}_2\text{TiAl}$  and  $\text{Co}_2\text{TiSn}$  was firstly scouted by Ishida et al. [12] using LDA method. But they are failure to observe half metallic ferromagnetism in these compounds. Kubler et al. [13] have resolved this complexity by analysis of formation and coupling of magnetic moment in the compounds  $\text{Co}_2\text{MnSn}$  and similarly Co-based alloys in the same year. They also represent the linear relationship between numbers of valence electrons and spin magnetic moment. Further, this relationship is main backbone of Slater-Pauling rule. According to this rule, if count of valence electron is equal to 24, then that compound shows zero magnetic moment and if, count of valence electron is different to 24, and then difference between the total number of valence electron and 24 represent the net amount of spin magnetic moment [14]. Kubler et al. [15] have observed in Co-based compound that there exists a straightforward relationship between Curie temperature and spin magnetic moment i.e. Curie temperature is directly proportional to the spin magnetic moment. Spintronics have vast area of application in the fields of magnetic memory device, magnetic sensor, tunnel junction, increased data processing speed, increased integration intensities and it also reduce the consumption of electricity [16-19]. Galanakis et al. [20] and Block et al. [21] have investigated the electronic and magnetic properties of a number of Heusler compounds and observed that most of them are half metallic and go along with Slater-Pauling rule. we are going to calculate the structural, electronic, optical, elastic and magnetic properties of  $\text{Co}_2\text{VZ}$  ( $Z = \text{Pb, Si, Sn}$ ) compounds, by using WIEN2k code and Atomistic Tool Kit-Virtual NanoLab (ATK-VNL) code within Generalized-gradient approximation (GGA) for exchange correlation functions.

### COMPUTATION DETAILS

The physical fundamental properties of full Heusler alloys have been performed by full-potential linearized augmented plane wave (FP-LAPW) [22] method incorporated in Wien2k code [23]. We have chosen suitable approximation of Perdew, Burke and Ernzerhof (PBE) [24-26] for regulate the exchange and correlation potential energy to the optimization of parameters like RKmax, K-Point and lattice constant and optimized energy. Spin orbit coupling effect was considered to perform all the calculations. Electronic structure calculations are accurately calculated by WIEN2k code for solids. Core states are considered relativistic and valence states are considered as semi-

relativistic way and energy between these two states (cut off parameter) was set -6.0Ry. In first Brillouin zone 1000 k-points have been used for this code. But we need to set the number of k-points for the calculation of optical properties and this new value of k-points used are 10000. The size of the basis sets are controlled by convergence or cutoff parameter, whose value is  $R_{mt} K_{max}$  set to 7.0. Here plane wave smallest radius of muffin-tin sphere is denoted by  $R_{mt}$  and maximum modulus for reciprocal lattice vector used in elaboration of flat wave function is denoted by  $K_{max}$ . The energy convergence criterion was taken as 0.0001Ry. To expand the spherical harmonics in the atomic sphere the value of angular momentum maximum ( $l_{max}$ ) is taken as 10. In the central region the charge density and potential were elaborated as a cheerier series with wave vector up to  $G_{max}=10$ . For the each atom muffin tin sphere radii ( $R_{MT}$ ) are tabulated in Table 1.

Table 1.

Muffin tin radius ( $R_{MT}$ ) for  $Co_2VZ$  ( $Z= Pb, Si, Sn$ ).

$R_{MT}$ (a.u.)	Compounds		
	$Co_2VPb$	$Co_2VSi$	$Co_2VSn$
Co	2.36	2.30	2.21
V	2.36	2.19	2.15
Z	2.48	1.91	2.21

Atomistic Tool Kit-Virtual NanoLab (ATK-VNL) package [27] is a Pseudo-potential method carried out in the framework of density functional theory (DFT) [28, 29]. It is a commercially licensed tool kit. Above mentioned properties have also investigated with the help of this tool kit. These calculations have been applied to investigate electronic and magnetic properties of  $Co_2VZ$  ( $Z= Pb, Si, Sn$ ) using Pulay Mixer algorithm [30]. For investigations, we have used double-zeta ( $\zeta$ ) polarized basis set for electron wave function expanding and GGA for exchange-correlation functional. The structures are permitted to optimize until each atom achieve force convergence criteria 0.05 eV/Å and maximum stress is 0.05 eV/Å<sup>3</sup>. Maximum numbers of step performed are 200 for the optimization and during this process maximum step size 0.2 Å is also fixed. Convergence is achieved by deciding mesh cutoff energy on the ground of convergence principle and for this computation 150 Ryd has been projected all over calculation as the most favorable after several convergence tests. For spin polarization, up and down initial state have been selected for the atoms. We used 10 x 10 x 10 Monkhorst-Pack k-mesh [31] for brillouin zone sampling to maintain balance between computational time and results accuracy. Further, all constrain in x, y and z directions are removed for optimization of structures.

## RESULTS AND DISCUSSIONS

### Structural parameters

Space group of full Heusler compound is 225 Fm-3m. The chemical formula for full Heusler is  $Co_2VZ$  ( $Z = Pb, Si, Sn$ ) having L2<sub>1</sub> structure showing their composition 2:1:1. Its structure is formed by three penetrating FCC-lattices with atomic positions at  $X_1$  (1/4, 1/4, 1/4),  $X_2$  (3/4, 3/4, 3/4),  $Y$  (1/2, 1/2, 1/2) and  $Z$  (0, 0, 0). Where X and Y atoms are transition metal and Z is main group metal or semimetal [32, 33]. The equation of state given by Murnaghan [34] gives the value of total energy and pressure as a function of volume is stated as:

$$E(V) = E_0 + \left[ \frac{BV}{B_p} \left( \frac{1}{(B_p - 1)} \left( \frac{V_0}{V} \right)^{B_p} + 1 \right) - \frac{BV_0}{(B_p - 1)} \right]$$

$$P(V) = \frac{B}{B_p} \left\{ \left( \frac{V_0}{V} \right)^{B_p} - 1 \right\},$$

where, Pressure ( $P$ ) =  $-\frac{dE}{dV}$ ,  $B_p = -V \frac{dP}{dV} = V \frac{d^2E}{dV^2}$

In the above equations  $E_0$  is the minimum energy at  $T = 0K$ ,  $B$  is the bulk modulus,  $B_p$  is the pressure derivative of the bulk modulus and  $V_0$  is the equilibrium volume. We perform the operation volume optimization for stable structure and their results are shown in Figure 1. Optimized lattice constant of WIEN2k and ATK-VNL are slightly differing from each other. Lattice constant in WIEN2k for the compounds  $Co_2VZ$  ( $Z= Pb, Si, Sn$ ) are slightly greater than the lattice constant optimized in ATK-VNL. Compared values of bulk modulus by these two codes reveals the results that value of bulk modulus of compounds  $Co_2VPb$  and  $Co_2VSn$  are less and Value of the compound  $Co_2VSi$  is more in WIEN2k code than ATK-VNL code. The compound  $Co_2VSi$  has showing largest value of bulk modulus in comparison to the others. Calculated values of the optimized lattice parameter, equilibrium energy and pressure derivative have been presented in Table 2.

Table 2.

Lattice parameter, Bulk modulus, Equilibrium energy and Pressure derivative for  $\text{Co}_2\text{VZ}$  ( $Z = \text{Pb, Si, Sn}$ ).

Compounds	Lattice Constants $a_0$ (Å)		Bulk modulus (GPa)		Equilibrium Energy (Ry)	Pressure derivative
	Calculated		Calculated			
	WIEN2k	ATK	WIEN2k	ATK		
$\text{Co}_2\text{VPb}$	6.125	6.073	179.50	195.74	-49329.729	6.872
$\text{Co}_2\text{VSi}$	5.685	5.638	234.36	233.94	-8052.753	5.406
$\text{Co}_2\text{VSn}$	6.021	5.957	186.08	206.20	-19830.786	1.851

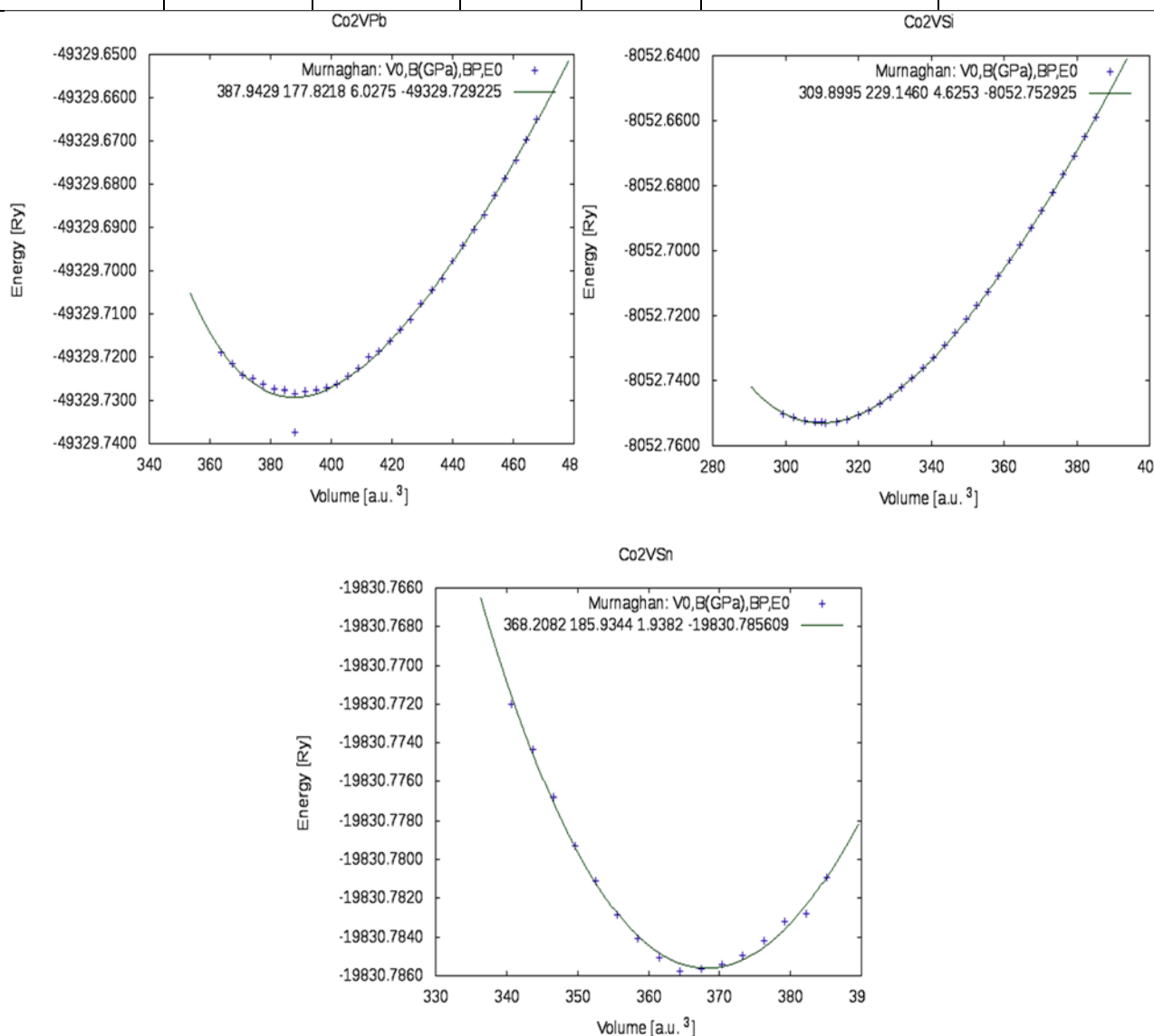


Figure 1. Volume optimization for the lattice parameters

### Electronic and magnetic properties

Due to spin of electron magnetic moment of a material can change. This change in magnetic moment is studied from the band structure and density of state of Heusler compounds. If that compound shows metallic behavior in one spin channel and semiconducting or insulating behavior in other spin channel at Fermi level then that compound is known as half metallic ferromagnetic representing 100% spin polarization. This phenomenon is known as Spin polarization. In the present era Spintronics is very interesting area of research. The advantages of Spintronics devices are nonvolatile magnetic memory, magnetic sensor, tunnel junction, increased data processing speed, increased integration intensities and processing speed of data is very high. These devices reduce electric power consumption and there is decrease in heat dissipation. Spin polarized calculations of  $\text{Co}_2\text{VZ}$  ( $Z = \text{Pb, Si, Sn}$ ) compounds within Generalized-gradient approximation (GGA) full Heusler have been carried out at the optimized lattice parameters. Intrinsic spin of electron is responsible for magnetic moment. Theoretical value of spin polarization can be calculated using the formula as given below.

$$P_n = \frac{n \uparrow - n \downarrow}{n \uparrow + n \downarrow}$$

If either  $n_{\uparrow} = 0$  or  $n_{\downarrow} = 0$ , then  $P_n = 1$  or  $-1$ . It means, if either up or down spin exists then the spin polarization is 100%. These types of materials are known as half metals ferromagnetic [35]. If the value of  $P_n$  is vanishes then the materials are paramagnetic or anti-ferromagnetic even below the magnetic transition temperature. The difference between the highest energy occupied point in valence band region and the lowest unoccupied energy point in conduction band is known as energy gap. Study of energy gap from DOS and band structure of the compounds  $\text{Co}_2\text{VZ}$  ( $Z = \text{Pb, Si, Sn}$ ) shows the result that out of three compounds only  $\text{Co}_2\text{VSi}$  does not show a band gap in minority spin channel through WIEN2k code and showing 100% spin polarization. Other two listed compound ( $\text{Co}_2\text{VPb}$  and  $\text{Co}_2\text{VSn}$ ) shows band gaps 0.33 eV and 0.54 eV, when code executed in WIEN2k and showing semiconducting behavior. Outcome of ATK-VNL code reveals that all three compound shows band gap in down spin and there is no any band gap observed in up spin channel. Obtained energy gap and spin polarization for the above full Heusler compound is summarized as under in Table 3. The detailed results of band structures and density of states are shown in Figures 2-5.

Table 3.

Energy gap and spin polarization for  $\text{Co}_2\text{VZ}$  ( $Z = \text{Pb, Si, Sn}$ )

Compounds	Energy gap $E_g$ (eV)				Spin polarization	
	WIEN2k		ATK		WIEN2k	ATK
	Up spin	Down spin	Up spin	Down spin		
$\text{Co}_2\text{VPb}$	0.0	0.33	0.0	-0.51	100%	100%
$\text{Co}_2\text{VSi}$	0.0	0.0	0.0	-0.82	$P_n$ vanishing	100%
$\text{Co}_2\text{VSn}$	0.0	0.54	0.0	-0.97	100%	100%

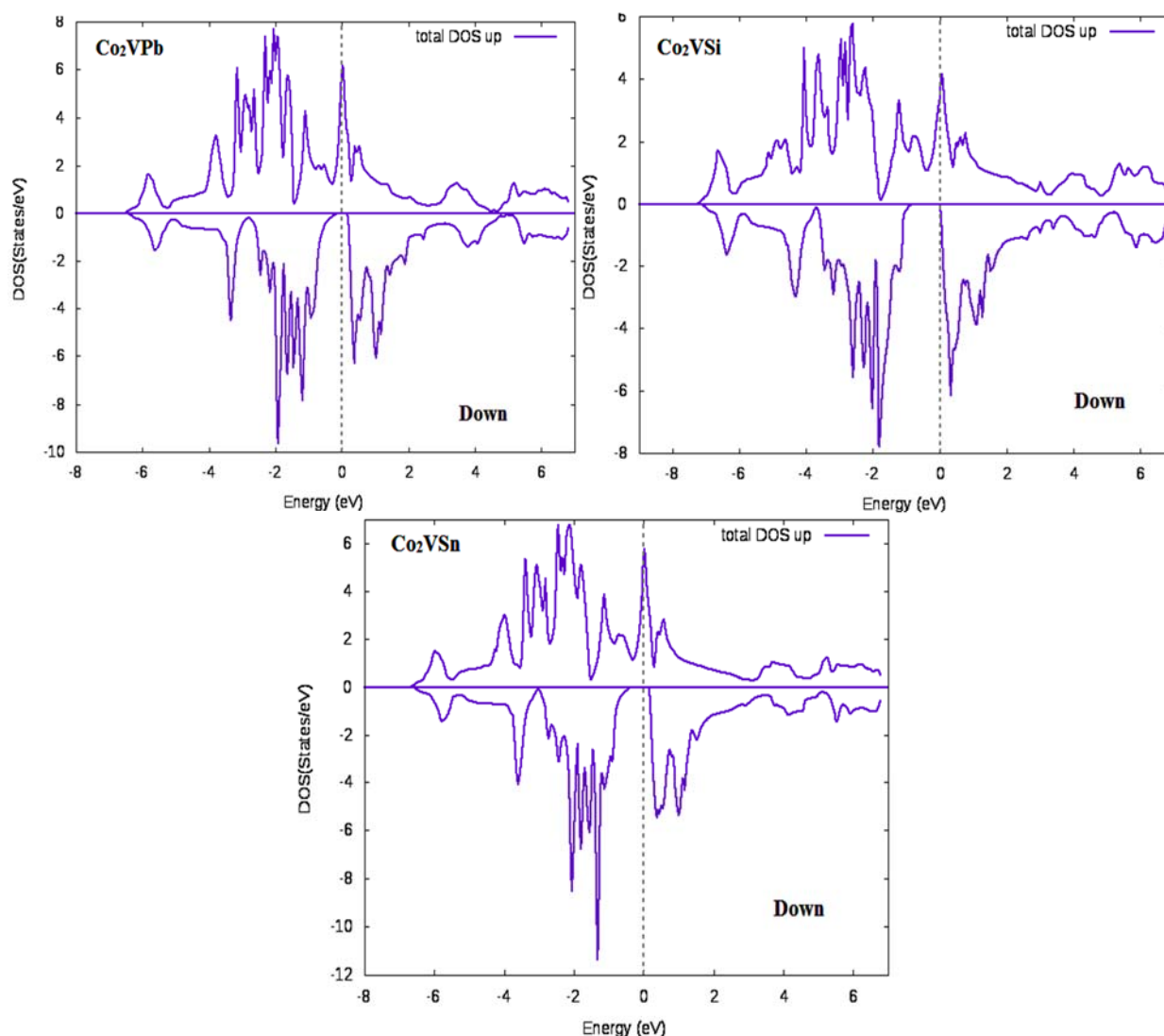


Figure 2. DOS of  $\text{Co}_2\text{VZ}$  ( $Z = \text{Pb, Si, Sn}$ ) using WIEN2K Code

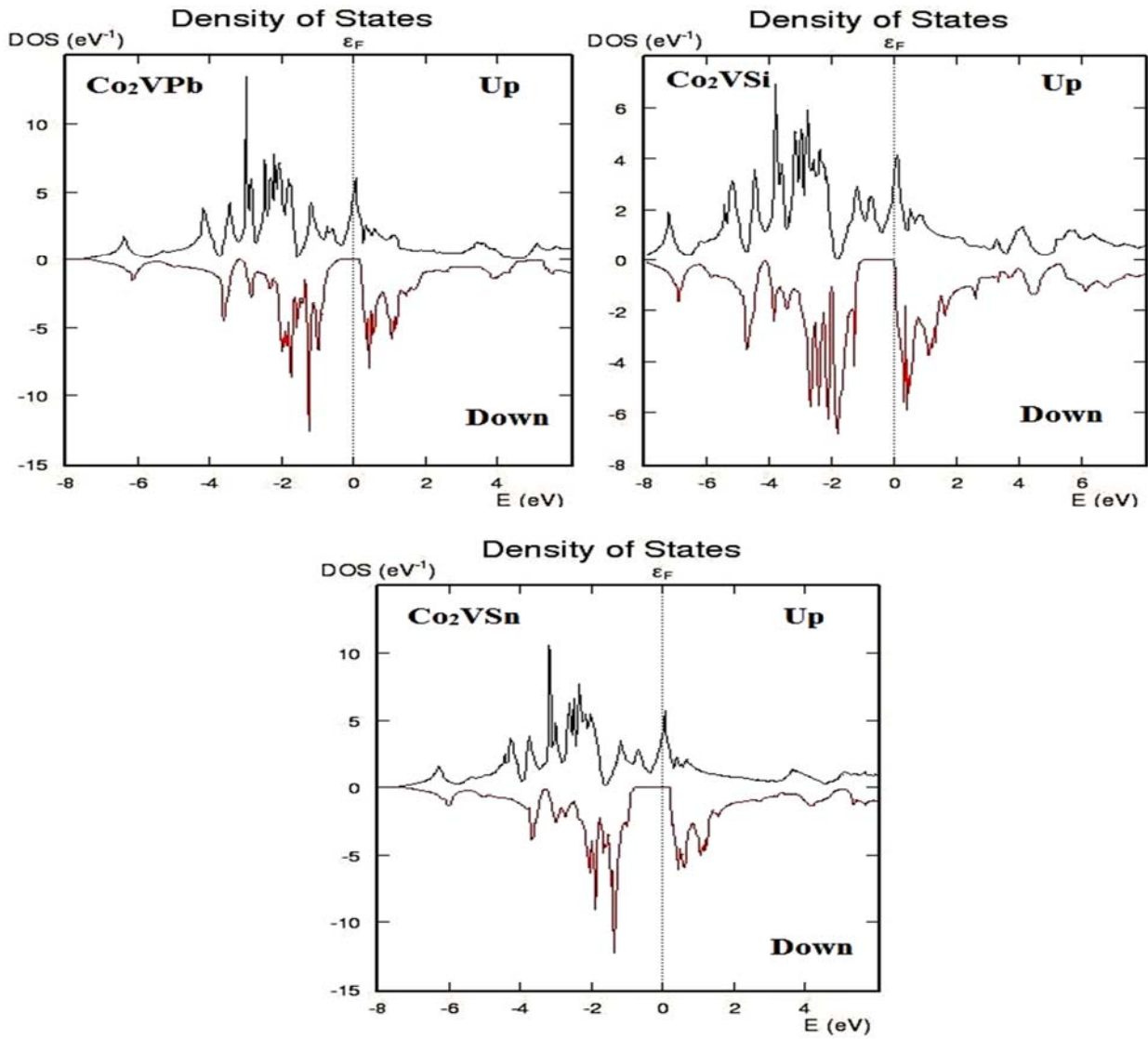


Figure 3. DOS of  $\text{Co}_2\text{VZ}$  ( $Z = \text{Pb, Si, Sn}$ ) using ATK-VNL Code.

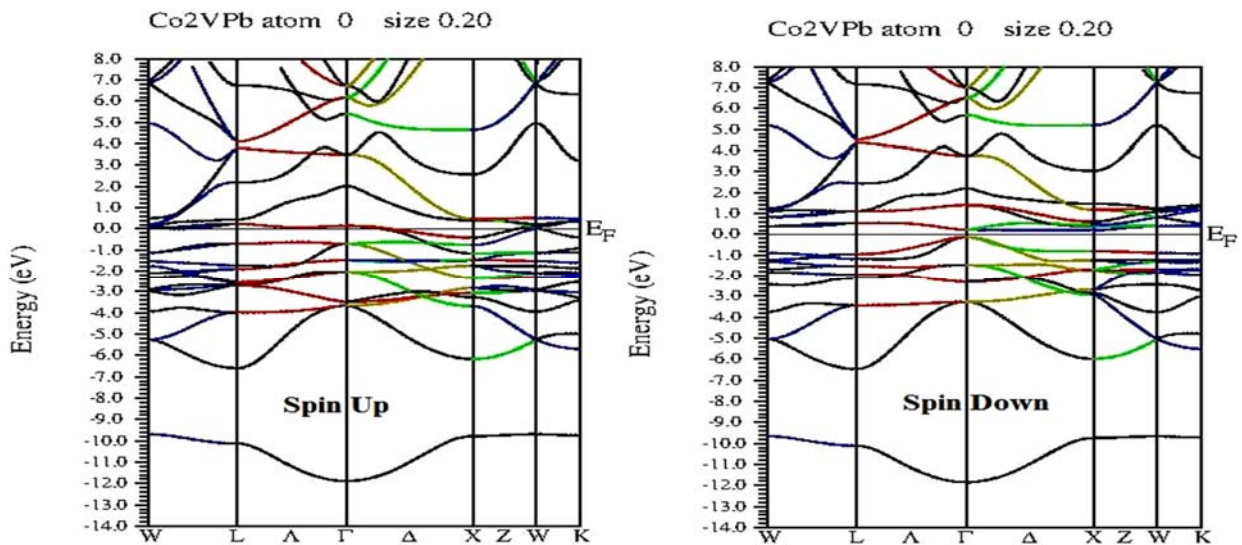


Figure 4. Band Structure of  $\text{Co}_2\text{VZ}$  ( $Z = \text{Pb, Si, Sn}$ ) using WIEN2K Code.  
(Continued on next page)

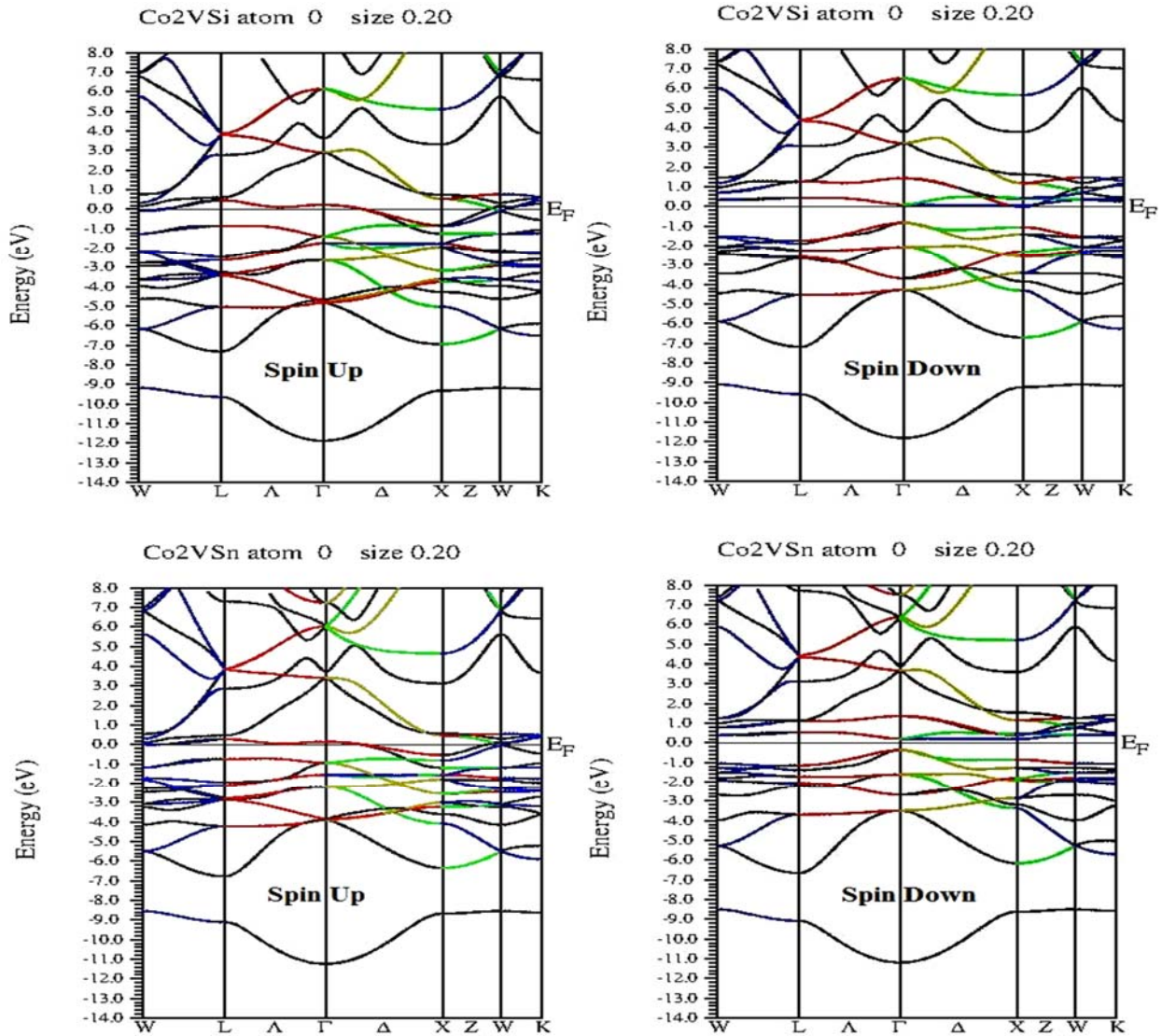


Figure 4. Band Structure of  $\text{Co}_2\text{VZ}$  ( $\text{Z} = \text{Pb, Si, Sn}$ ) using WIEN2K Code.  
(Continuation)

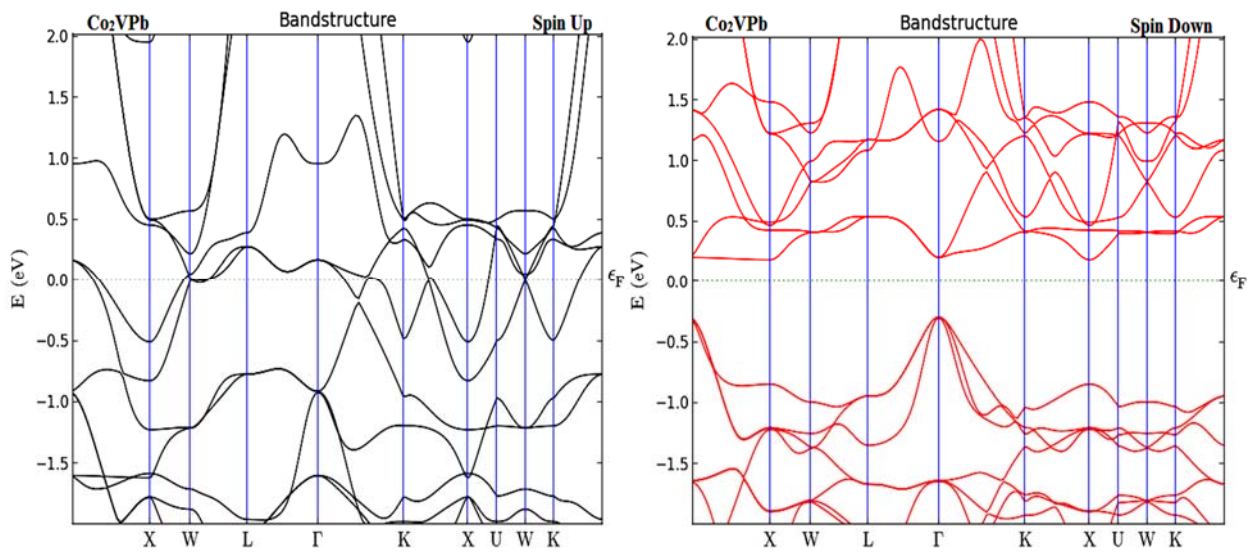


Figure 5. Band Structure of  $\text{Co}_2\text{VZ}$  ( $\text{Z} = \text{Pb, Si, Sn}$ ) using ATK-VNL Code.  
(Continued on next page)

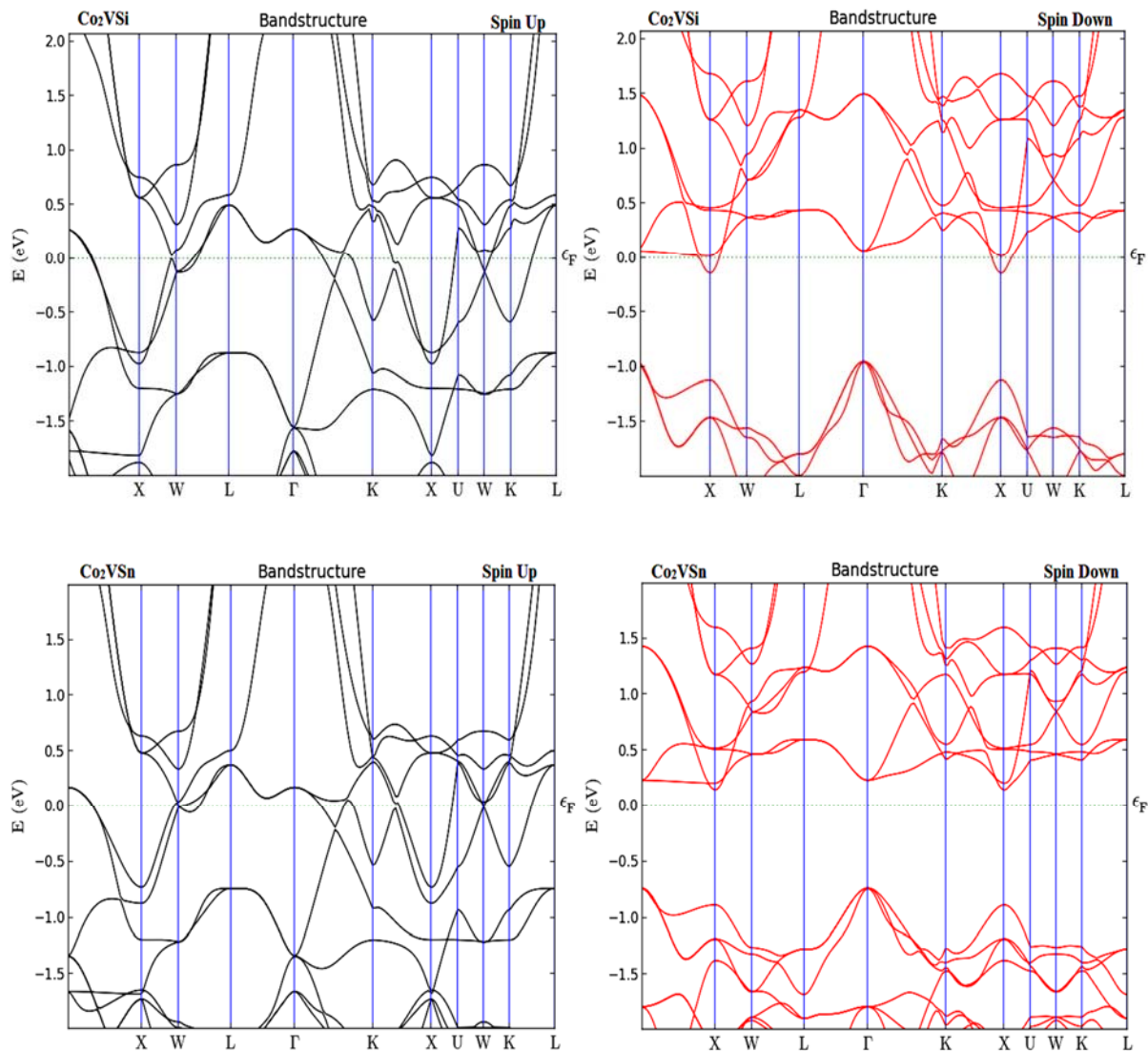


Figure 5. Band Structure of  $\text{Co}_2\text{VZ}$  ( $Z = \text{Pb, Si, Sn}$ ) using ATK-VNL Code  
(Continuation)

There is a linear relationship between numbers of valence electrons and spin magnetic moment. This simple relationship is main clue of Slater-Pauling rule. J. C. Slater [36] and L. Pauling [37] derive a formula for calculating the magnetic moment per unit cell theoretically and that formula is known as Slater-Pauling rule. According to this rule, if count of valence electrons in full Heusler compounds is equal to 24, then that compound shows zero magnetic moment and if, count of valence electron is different to 24, and then difference between the total number of valence electron and 24 represent the net amount of spin magnetic moment per unit cell. This theoretical method of prediction of magnetic moment is provided by Slater-Pauling. Method for Full Heusler compound is given as-

$$M_t = Z_t - 24$$

Where,  $M_t$  denotes the total magnetic moment per unit cell and  $Z_t$  denotes the total count of valence electron. Full Heusler compounds have a straightforward relationship between Curie temperature and spin magnetic moment i.e. Curie temperature is directly proportional to the spin magnetic moment. For the ferromagnetic half-metallic Heusler compounds, the Curie temperature increases by  $\sim 175$  K per added electron after 24. Here, the results obtained by the codes WIEN2k and ATK-VNL are compared with results derived from theoretical method Slater-Pauling rule. For analysis the values of magnetic moment from WIEN2k, ATK-VNL code and Slater-Pauling rule, table 4 is very helpful for us. Total number of valence electrons for all the three compounds  $\text{Co}_2\text{CrZ}$  ( $Z = \text{In, Sb, Sn}$ ) is 27. So magnetic moments per unit cell for all three compounds from Slater-Pauling rule is  $3.0 \mu_B$ . Now, the results derived by WIEN2k and ATK-VNL are 3.00 and 3.00, 3.02 and 2.96, 3.00 and 3.00 respectively. These compiled values are equal to the values of theoretical method Slater-Pauling, except slight difference between the values of  $\text{Co}_2\text{VSi}$ . So, these listed compounds have nice agreement with Slater-Pauling behavior. Investigation of results reveals that Co and Cr position atom contribute major section of magnetic moment and small amount of magnetic moment contribution is due to Z position atom. The

calculated results for magnetic moments for Co<sub>2</sub>VZ (Z= Pb, Si, Sn) obtained using full potential linearized augmented plane wave (FP-LAPW) method implemented in WIEN2k and pseudo-potentials method implemented in Atomistic Tool Kit-Virtual NanoLab (ATK-VNL) within Generalized- gradient approximation (GGA) for exchange correlation functions is tabulated in Table 4.

Table 4.

Total magnetic moments of the compounds Co<sub>2</sub>VZ (Z= Pb, Si, Sn).

Compounds	Z <sub>t</sub>	Magnetic moment (μ <sub>B</sub> )		
		WIEN2k	ATK	Slater-Pauling (Z <sub>t</sub> - 24)
Co <sub>2</sub> VPb	27	3.00	3.00	3.00
Co <sub>2</sub> VSi	27	3.02	2.96	3.00
Co <sub>2</sub> VSn	27	3.00	3.00	3.00

### Optical properties

Before fabrication of optoelectronics devices, it is compulsory to understand the optical properties of a material whether it can be used for it or not. For it, we need to study some optical properties like as dielectric function, optical conductivity, reflectivity, excitation coefficient, absorption coefficient and electron energy loss as a function of photon energy for a given material. Present section describes such optical properties of the compounds Co<sub>2</sub>VZ (Z= Pb, Si, Sn). When an electromagnetic radiation is fall on a material then optical response of that material is described by complex dielectric function. This complex dielectric function can be written in the form of as below.

$$\epsilon(m) = \epsilon_1(m) + i\epsilon_2(m)$$

Where  $\epsilon_1(m)$  real represents polarization of material when electric field is applied and absorption in a material or loss of energy into the medium is described by ( $\epsilon_2(m)$ ) imaginary part of complex dielectric function [38, 39]. It is considered that the transitions exist from occupied to unoccupied bands for explain the optical spectra. Inter-band region is chosen for studying the optical properties. The optical spectra for different optical properties are shown in Figure 6(a-h).

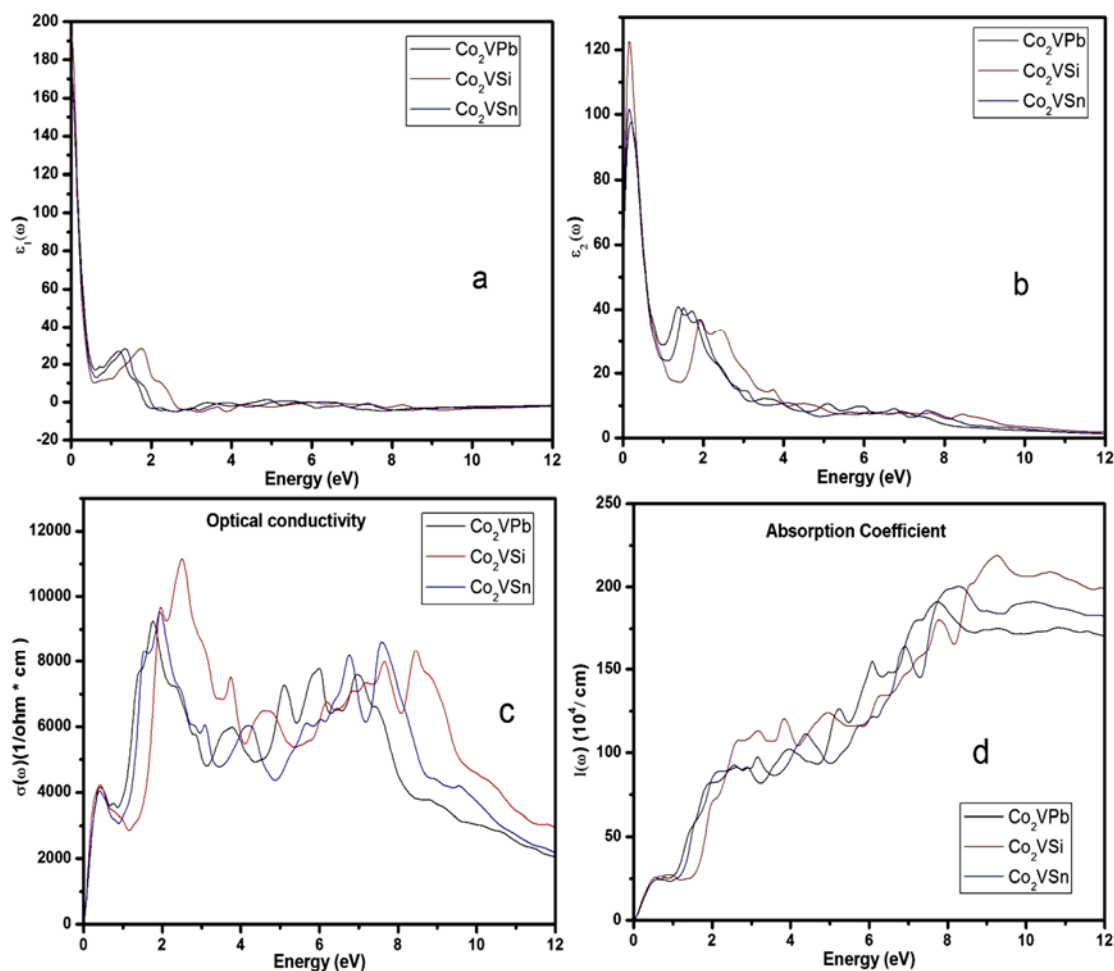


Figure 6. Calculated optical parameters (a) real part of dielectric function, (b) imaginary part of dielectric function, (c) optical conductivity, (d) absorption coefficient, (e) electron energy-loss function, (f) reflectivity, (g) refractive index and (h) extinction coefficient for Co<sub>2</sub>VZ (Z= Pb, Si, Sn).

(Continued on next page)



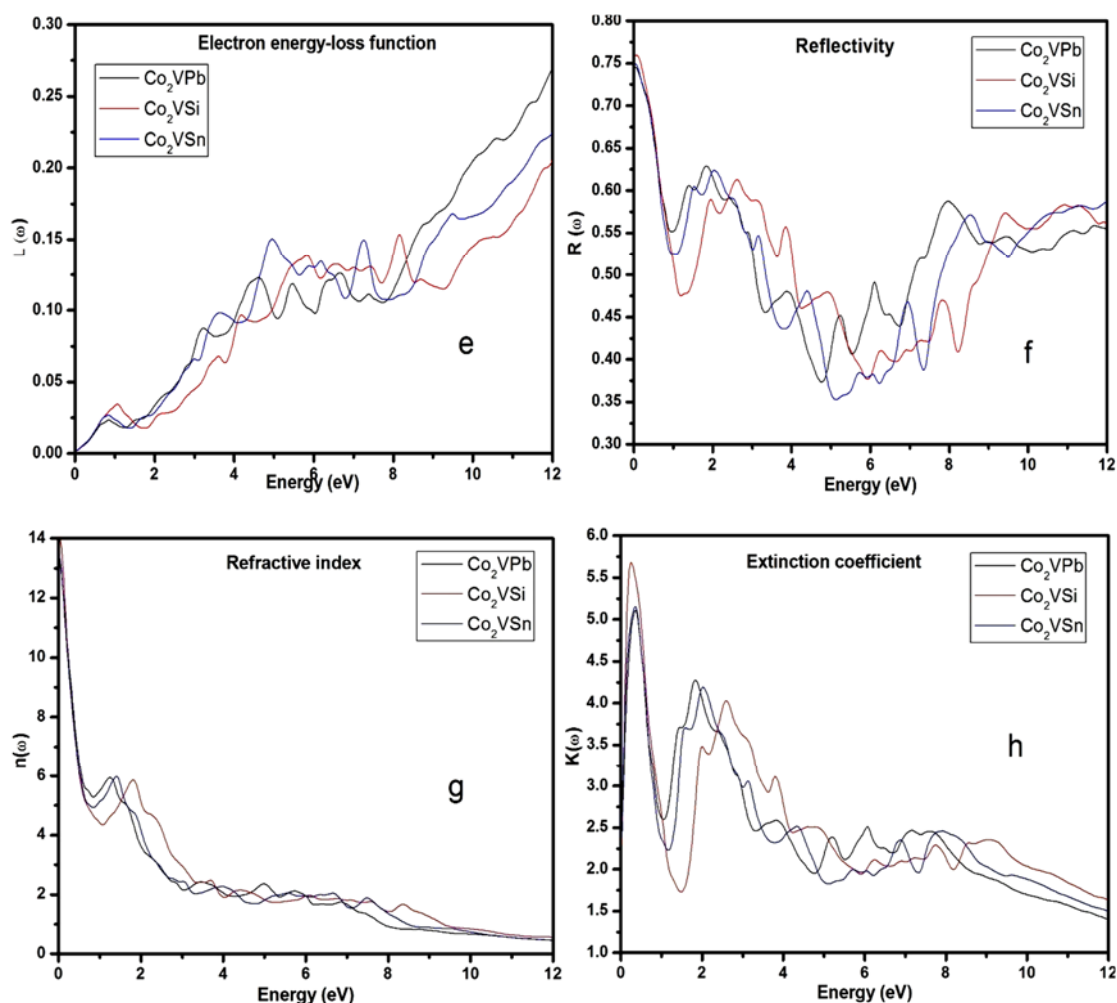


Figure 6. Calculated optical parameters (a) real part of dielectric function, (b) imaginary part of dielectric function, (c) optical conductivity, (d) absorption coefficient, (e) electron energy-loss function, (f) reflectivity, (g) refractive index and (h) extinction coefficient for  $\text{Co}_2\text{VZ}$  ( $Z = \text{Pb, Si, Sn}$ ).

(Continuation)

The main peaks of imaginary part of dielectric function are obtained in infrared region from 0.08 to 0.30 eV. After that, imaginary part of dielectric function decreases rapidly and some small peaks are observed near visible region. The values of zero frequency real ( $\epsilon_1(\omega)$ ) and imaginary part ( $\epsilon_2(\omega)$ ) of complex dielectric functions are 170.514 and 58.983, 192.316 and 64.438, 174.193 and 63.898 for the compounds  $\text{Co}_2\text{VZ}$  ( $Z = \text{Pb, Si, Sn}$ ) respectively as investigated from the Figure 6 (a) and 6 (b). Due to electromagnetic field, value of conduction of electron is described by optical conductivity. Figure 6(c) gives a graphical representation of optical conductivity. In this graphical view, sharp peaks are shown in visible region and highest sharp peak is obtained at 2.48 eV by  $\text{Co}_2\text{VSi}$  representing more conduction of electron as compared with other two compound. The value of absorption of photon is described by absorption coefficient means more value of absorption coefficient more photons are absorbed by the material. As we increase the values of energy from infrared region to ultraviolet region then value of absorption coefficient is also increases as shown in the figure 6 (d). Maximum value of photon absorption is found at 9.26 eV by  $\text{Co}_2\text{VSi}$  showing highest peak out of three compounds. When fast moving electron passes through a medium then there is loss in energy of fast-moving electron. This loss of fast-moving electron can be calculated by electron energy-loss function graph. Like absorption coefficient, value of electron energy – loss function is also increasing as we increase the value of energy as shown in figure 6 (e). From figure 6 (f), we observe the values of zero frequency reflectivity which are 0.745, 0.758 and 0.749 for the compounds  $\text{Co}_2\text{VZ}$  ( $Z = \text{Pb, Si, Sn}$ ) respectively. This optical property gives the values of reflection when electromagnetic radiation is fall on the surface of a material. The region in which material substantially absorbs light and it cannot effectively reflect light in the same span. The plasma frequency is the frequency corresponding to plasma resonance at which sharp peaks are associated. As if the frequency is above the plasma frequency then the material showing the dielectric behavior and below which the material shows metallic behavior. Due to wide applications of refractive index, it is most valuable to analyses; because it determines the dispersive power of prisms, focusing power of lenses, light guiding, and critical angle for total internal reflection etc. The values for zero frequency refractive index for the compounds  $\text{Co}_2\text{VZ}$  ( $Z = \text{Pb, Si, Sn}$ ) were calculated as 13.246, 14.056 and 13.412 respectively. Figure 6(h) gives the graphical representation of extinction coefficient

spectrum. A notable narrow peak is shown in the infrared region along the range 0.18 to 0.50eV and then value of extinction coefficient is decreases. Near to visible region further a small broad peak is observed between 1.826 – 2.65eV and further value is decreases in the ultraviolet region.

### Elastic properties

Elastic properties are the most fundamental properties of the material calculated using first principle method. Cubic crystal elasticity is determined by three reduced elastic constants  $C_{11}$ ,  $C_{12}$  and  $C_{44}$ , out of six independent constant. These three reduced elastic constant gives us very important information about structure stability, mechanical properties, bond indexes and anisotropy of material. The crystal must satisfy the traditional mechanical stability condition of elastic constant. The traditional mechanical stability condition for cubic crystal is as below [40, 41].

$$C_{11} - C_{12} > 0, C_{11} > 0, C_{11} + 2C_{12} > 0, C_{44} > 0, C_{12} < B < C_{11}$$

Structural stability is obtained by anisotropic factor, which is denoted by ‘A’ if the value of ‘A’ is equal to one then material is isotropic and if the value of ‘A’ deviate from one then material is anisotropic. A property of material which does not depend on the direction is known as isotropic.

$$A = \frac{2C_{44}}{C_{11} - C_{12}}$$

Stiffness and flexibility of a material can be determined by bond index via Cauchy pressure, which is expressed as  $C_P = C_{12} - C_{44}$ . From this relation if the value is positive, then the material is metallic in nature and if value is negative, then the material is nonmetallic. Further, positive result shows ductile nature material and negative result shows brittle nature of material. If the value of bond index is less than 12 shows soft material and greater than 12 shows hard material [42]. Pugh’s ratio B/G is also used for to explain the material is brittle or ductile. If the B/G ratio is less than 1.75 then material is brittle type and if this ratio B/G is greater than 1.75 then it is ductile. Mechanical properties of the compounds are determined by Bulk modulus (B), young modulus (E), Shear modulus (G) and Poisson ratio ( $\nu$ ) by Voigt-Reuss-Hill (VRH) averaging method [43-44]. Formulas for B, E, G and  $\nu$  by using elastic constant can be expressed as.

$$B = B_V = B_R = \frac{C_{11} + 2C_{12}}{3}$$

$$G = \frac{G_V + G_R}{2}$$

$$G_V = \frac{C_{11} - C_{12} + 3C_{44}}{5}$$

$$G_R = \frac{5C_{44} (C_{11} - C_{12})}{[4C_{44} + 3(C_{11} - C_{12})]}$$

(V = Voigt and R = Reuss)

Young modulus is also used to determine the stiffness of material. This can be obtained in term of B and G.

$$E = \frac{9BG}{3B + G}$$

The value of Poisson ratio can be calculated in term of B and G. The values of Poisson ratio lie between 0 - 0.5 for most of the material.

$$\nu = \frac{3B - 2G}{2(3B + G)}$$

We use here Atomistic Tool Kit-Virtual NanoLab (ATK-VNL) package using Pseudo-potential method carried out in the framework of density functional theory (DFT). All the results carried out from this code are assembled in table 5.

Table 5.

Elastic constants and bulk modulus B (GPa), shear modulus G (GPa), Young’s modulus E (GPa), B/G values, Poisson’s ratio ( $\nu$ ) and anisotropy factor (A) of  $Co_2VZ$  (Z= Pb, Si, Sn) compounds.

Compound	Elastic constants (GPa)			B (GPa)	G (GPa)	E (GPa)	B/G	$\nu$	A
	$C_{11}$	$C_{12}$	$C_{44}$						
$Co_2VPb$	228.51	179.36	85.22	195.74	51.93	70.77	3.77	0.44	3.47
$Co_2VSi$	271.49	215.17	137.88	233.95	73.94	81.22	3.16	0.44	4.90
$Co_2VSn$	245.91	186.36	106.81	206.21	64.24	85.22	3.21	0.43	3.59

From the Table 5, we have observed that traditional mechanical stability condition  $C_{11} - C_{12} > 0, C_{11} > 0, C_{11} + 2C_{12} > 0, C_{44} > 0, C_{12} < B < C_{11}$  for all the compounds  $Co_2VZ$  (Z= Pb, Si, Sn) is satisfied. Results of anisotropic

constant 'A' are deviated from one for all three compounds. We have concluded that the compounds Co<sub>2</sub>VZ (Z= Pb, Si, Sn) are anisotropic in nature. Values of Poisson are lie between zero to 0.5. Table 5 reveals that, Pugh's ratio B/G is greater than 1.75 for all compounds recorded in table. These materials are ductile in nature. Values of Cauchy pressure ( $C_p = C_{12} - C_{44}$ ) compiled from the table 5 are positive for these compounds Co<sub>2</sub>VZ (Z= Pb, Si, Sn) and shows metallic nature.

### SUMMARY AND CONCLUSIONS

We have compiled the results for Structural, electronic, optical and magnetic properties of Co<sub>2</sub>VZ (Z= Pb, Si, Sn) compounds by two simulation codes. From this study, we have analyzed that out of three compounds, two compounds show half metallicity and 100% spin polarization with L<sub>21</sub> ordered stable structures except Co<sub>2</sub>VSi in full potential linearized augmented plane wave (FP-LAPW) method. But results of pseudo-potentials method reveals that all three compounds show half metallicity and 100% spin polarization with L<sub>21</sub> ordered stable structures. Calculated magnetic moments per unit cell have good agreement with the Slater-Pauling behavior. Optical spectra of these compounds named as reflectivity, refractive index, excitation coefficient, absorption coefficient, optical conductivity and electron energy loss have been analyzed. Values of absorption coefficient and electron energy - loss function are increases as we increase the value of energy. The predicted results shows that the compounds Co<sub>2</sub>VZ (Z= Pb, Sn) are suitable for Spintronics applications. Compilation of elastic properties presented that the above listed compounds are ductile and metallic in nature.

### ORCID IDs

 Sukhender, <https://orcid.org/0000-0002-2149-5669>;  Lalit Mohan, <https://orcid.org/0000-0003-3323-8296>  
 Pravesh Pravesh, <https://orcid.org/0000-0002-0876-4836>;  Ajay Singh Verma, <https://orcid.org/0000-0001-8223-7658>

### REFERENCES

- [1] Y. Ohnuma, M. Matsuo, and S. Maekawa, Phys. Rev. B. **94**, 184405 (2016), <https://doi.org/10.1103/PhysRevB.94.184405>.
- [2] S.M. Griffin, and J.B. Neaton, Prediction of a new class of half-metallic ferromagnets from first principles. Phys. Rev. Mater. **1**, 044401 (2017) <https://doi.org/10.1103/PhysRevMaterials.1.044401>.
- [3] N.I. Kourov, V.V. Marchenkov, K.A. Belozerova, and H.W. Weber, J. Exper. Theor. Phys. **118**, 426-431 (2014), <https://doi.org/10.1134/S1063776114020137>.
- [4] M. Sun, Q. Ren, Y. Zhao, S. Wang, J. Yu, and W. Tang, J. Appl. Phys. **119**, 143904 (2016), <https://doi.org/10.1063/1.4945771>.
- [5] I. Galanakis, K. Özdoğan, and E. Şaşıoğlu, AIP Adv. **6**, 055606 (2016), <https://doi.org/10.1063/1.4943761>.
- [6] Y. Wang, R. Ramaswamy, and H. Yang, J. Phys. D. Appl. Phys. **51**, 273002 (2018), <https://doi.org/10.1088/1361-6463/aac7b5>.
- [7] Y. Feng, Z. Cui, M. S. Wei, and B. Wu, Appl. Surf. Sci. **499**, 78-83 (2019), <https://doi.org/10.1016/j.apsusc.2018.09.247>.
- [8] R.A. de Groot, F.M. Muller, P.G. Van Engen, and K.H.J. Buschow, Phys. Rev. Lett. **50**, 2024-2027 (1983), <https://doi.org/10.1103/PhysRevLett.50.2024>.
- [9] A. Aguayo, and G. Murrieta, J. Magnetism and Magnetic Materials, **323**, 3013-3017 (2011), <https://doi.org/10.1016/j.jmmm.2011.06.038>.
- [10] G. Fiedler, and P. Kratzer, Phys. Rev. B. **94**, 075203 (2016), <https://doi.org/10.1103/PhysRevB.94.075203>.
- [11] C.K. Barman, and A. Alam, Phys. Rev. B. **97**, 075302 (2018), <https://doi.org/10.1103/PhysRevB.97.075302>.
- [12] S. Ishida, S. Akazawa, Y. Kubo, J. Ishida, J. Phys. F: Met. Phys. **12**, 1111 (1982), <https://doi.org/10.1088/0305-4608/12/6/012>.
- [13] J. Kübler, A.R. William, and C.B. Sommers, Phys. Rev. B **28**, 1745-1755 (1983), <https://doi.org/10.1103/PhysRevB.28.1745>.
- [14] Y. Miura, K. Nagao, and M. Shirai, Phys. Rev. B **69**, 144413 (2004), <https://doi.org/10.1103/PhysRevB.69.144413>.
- [15] J. Kübler, G.H. Fecher, and C. Felser, Phys. Rev. B **76**, 024414 (2007), <https://doi.org/10.1103/PhysRevB.76.024414>.
- [16] S.A. Wolf, D.D. Awschalom, R.A. Buhrman, J.M. Daughton, S.V. Molnar, M.L. Roukes, A.Y. Chtchelkanova, and D.M. Treger, Science, **294**, 1488-1495 (2001), <https://doi.org/10.1126/science.1065389>.
- [17] E. Şaşıoğlu, L.M. Sandratskii, P. Bruno, I. Galanakis, Phys. Rev. B. **72**, 184415 (2005), <https://doi.org/10.1103/PhysRevB.72.184415>.
- [18] S. Wurmehl, G.H. Fecher, H.C. Kandpal, V. Ksenofontov, C. Felser, H. Lin, Appl. Phys. Lett. **88**, 032503 (2006), <https://doi.org/10.1063/1.2166205>.
- [19] I. Galanakis, J. Phys.: Condens. Matter, **14**, 6329-6340 (2002), <https://doi.org/10.1088/0953-8984/14/25/303>.
- [20] I. Galanakis, P.H. Dederichs, and N. Papanikolaou, Phys. Rev. B **66**, 134428 (2002), <https://doi.org/10.1103/PhysRevB.66.134428>.
- [21] T. Block, C. Felser, G. Jakob, J. Ensling, B. Muhling, P. Gutlich, V. Beaumont, F. Studer, and R.J. Cava, J. Solid State Chem. **176**, 646-651 (2003), <https://doi.org/10.1016/j.jssc.2003.07.002>.
- [22] E. Wimmer, H. Krakauer, M. Weinert, and A.J. Freeman, Phys. Rev. B, **24**, 864-875 (1981), <https://doi.org/10.1103/PhysRevB.24.864>.
- [23] P. Blaha, K. Schwarz, G.K.H. Madsen, D. Kvasnicka, and J. Luitz, in: *WIEN2k, An Augmented Plane Wave + Local Orbitals Program for Calculating Crystal Properties*, edited by K. Schwarz, (Technical Universitatwien, Austria, 2001).
- [24] J.P. Perdew, K. Burke, and M. Ernzerhof, Phys. Rev. Lett. **77**, 3865-3868 (1996), <https://doi.org/10.1103/PhysRevLett.77.3865>.
- [25] J.P. Perdew, K. Burke, and Y. Wang, Phys. Rev. B. **54**, 16533 (1996), <https://doi.org/10.1103/PhysRevB.57.14999>.
- [26] E. Sjöstedt, L. Nordstrom and D.J. Singh, Solid State Commun. **114**, 15-20 (2000), [https://doi.org/10.1016/S0038-1098\(99\)00577-3](https://doi.org/10.1016/S0038-1098(99)00577-3).
- [27] *Atomistix ToolKit-Virtual Nanolab (ATK-VNL), QuantumWise Simulator, Version. 2014.3*, <http://quantumwise.com/>
- [28] Y.J. Lee, M. Brandbyge, J. Puska, J. Taylor, K. Stokbro, and M. Nieminen, Phys. Rev. B, **69**, 125409 (2004), <https://doi.org/10.1103/PhysRevB.69.125409>.
- [29] K. Schwarz, J. Solid State Chem. **176**, 319-328 (2003), [https://doi.org/10.1016/S0022-4596\(03\)00213-5](https://doi.org/10.1016/S0022-4596(03)00213-5).
- [30] P. Pulay, J. Comput. Chem. **3**, 556-560 (1982), <https://doi.org/10.1002/jcc.540030413>.
- [31] H.J. Monkhorst, and J.D. Pack, Phys. Rev. B, **13**, 5188-5192 (1976), <https://doi.org/10.1103/PhysRevB.13.5188>.
- [32] P.J. Webster, J. Phys. Chem. Sol. **32**, 1221-1231 (1971), [https://doi.org/10.1016/S0022-3697\(71\)80180-4](https://doi.org/10.1016/S0022-3697(71)80180-4).

- [33] Fr. Heusler, Ueber magnetische Manganlegierungen. Verh. Dtsch. Phys. Ges. **5**, 219 (1903).
- [34] F.D. Murnaghan, Proc. Natl. Acad. Sci. U.S.A. **30**, 244-247 (1944), <https://dx.doi.org/10.1073%2Fpnas.30.9.244>.
- [35] R.J. Soulen Jr., J.M. Byers, M.S. Osofsky, B. Nadgorny, T. Ambrose, S.F. Cheng, P.R. Broussard, C.T. Tanaka, J. Nowak, J.S. Moodera, A. Barry, and J.M.D. Coey, Science **282**, 85-88 (1998), <https://doi.org/10.1126/science.282.5386.85>.
- [36] J. C. Slater, Phys. Rev. **49**, 537-545 (1936), <https://doi.org/10.1103/PhysRev.49.537>.
- [37] L. Pauling, Phys. Rev. **54**, 899-904 (1938), <https://doi.org/10.1103/PhysRev.54.899>.
- [38] Y.V. Kudryavtsev, N.V. Uvarov, V.N. Iermolenko, and J. Dubowik, J. Appl. Phys. **108**, 113708 (2010), <https://doi.org/10.1063/1.3511433>.
- [39] N.V. Uvarov, Y.V. Kudryavtsev, A.F. Kravets, A.Ya. Vovk, R.P. Borges, M. Godinho, and V. Korenivski, J. Appl. Phys. **112**, 063909 (2012), <https://doi.org/10.1063/1.4752870>.
- [40] M. Born, and K. Huang, *Dynamical Theory of Crystal Lattices*, (Oxford, Clarendon, 1956), pp. 420.
- [41] A. Akriche, H. Bouafia, S. Hiadsi, B. Abidri, B. Sahli, M. Elchikh, M.A. Timaoui, B. Djebour, J. Magnetism and Magnetic Materials. **422**, 13-19 (2017), <https://doi.org/10.1016/j.jmmm.2016.08.059>.
- [42] D.G. Pettifor, J. Mater. Sci. Technol. **8**, 345-349 (1992), <https://doi.org/10.1179/mst.1992.8.4.345>.
- [43] R. Hill, Proc. Phys. Soc., A **65**, 349-354 (1952), <https://doi.org/10.1088/0370-1298/65/5/307>.
- [44] A. Hamidani, B. Bennecer, B. Boutarfa, Materials Chemistry and Physics. **114**, 732-735 (2009), <https://doi.org/10.1016/j.matchemphys.2008.10.038>.

**ПЛАСТИЧНА І МЕТАЛЕВА ПРИРОДА КОМПАУНДІВ ХЕЙСЛЕРА  $\text{Co}_2\text{VZ}$  ( $\text{Z} = \text{Pb, Si, Sn}$ ):  
БАЗОВІ ПРИНЦИПИ ДОСЛІДЖЕННЯ**

Сухендер<sup>а</sup>, Правеш Правеш<sup>б</sup>, Лаліт Мохан<sup>а</sup>, Аджай Сінгх Верма<sup>а</sup>

<sup>а</sup>Фізичний факультет, Банастхалі Відьяпіт, Банастхалі 304022, Індія

<sup>б</sup>Факультет електроніки і техніки зв'язку, група установ КІЕТ

Газибад, Уттар-Прадеш (Індія) 201206

У цій роботі оптикоелектронні, пружні і магнітні властивості  $\text{L}_{21}$  структурованих сполук Хейслера  $\text{Co}_2\text{VZ}$  ( $\text{Z} = \text{Pb, Si, Sn}$ ) були досліджені двома методами. Одним з них є метод повнопотенціальної лінеаризованої розширеної плоскої хвилі (FP-LAPW), реалізований в WIEN2k, а другим - метод псевдопотенціалу, реалізований в Atomistic Tool Kit-Virtual NanoLab (ATK-VNL). Всі ці сполуки показують нульову ширину забороненої зони в основному спіновому каналі в обох кодах моделювання, і кінцева заборонена зона становить 0,33 і 0,54 еВ в сплавах  $\text{Co}_2\text{VZ}$  ( $\text{Z} = \text{Pb, Sn}$ ) (напівпровідникових) відповідно. Причина в невеликому спіновому каналі поблизу рівня Фермі, що реалізовано в коді WIEN2k зі 100% спінової поляризацією, за винятком  $\text{Co}_2\text{VSi}$  (металік) з нульовою шириною забороненої зони. Ці сполуки виявилися ідеально напівметалевими ферромагнетиками (НМФ). Однак вищезгадані сполуки показують кінцеві заборонені зони в коді ATK-VNL. Розрахований магнітний момент цих з'єднань  $\text{Co}_2\text{VZ}$  ( $\text{Z} = \text{Pb, Si, Sn}$ ) становить 3,00 і 3,00, 3,02 і 2,96, 3,00 і 3,00 мВ в кодах WIEN2k і ATK-VNL відповідно. Таким чином, ми спостерігали, що обчислені значення за цими кодами моделювання і правилом Слейтера-Полінга добре налаштовуються. Були проаналізовані оптичні властивості цих сполук, такі як відбивна здатність, показник заломлення, коефіцієнт збудження, коефіцієнт поглинання, оптична провідність і енергетичні втрати електронів. Коефіцієнт поглинання і значення функції енергетичних втрат електронів збільшуються у міру збільшення енергії. Співвідношення  $\text{P}_{\text{в}}/\text{G}$  перевищує 1,75 для всіх з'єднань і показує пластичну природу з позитивним значенням тиску Коші ( $\text{CP} = \text{C}_{12} - \text{C}_{44}$ ) і показує металеву поведінку сполук  $\text{Co}_2\text{VZ}$  ( $\text{Z} = \text{Pb, Si, Sn}$ ).

**КЛЮЧОВІ СЛОВА:** напівметалевий ферромагнетик, заборонена зона, спинтроніка, магнітний момент, пружні постійні

**ПЛАСТИЧНАЯ И МЕТАЛЛИЧЕСКАЯ ПРИРОДА КОМПАУНДА ХЕЙСЛЕРА  $\text{Co}_2\text{VZ}$  ( $\text{Z} = \text{Pb, Si, Sn}$ ):  
БАЗОВЫЕ ПРИНЦИПЫ ИССЛЕДОВАНИЯ**

Сухендер<sup>а</sup>, Правеш Правеш<sup>б</sup>, Лалит Мохан<sup>а</sup>, Аджай Сингх Верма<sup>а</sup>

<sup>а</sup>Физический факультет, Банастхали Видьяпит, Банастхали, 304022, Индия

<sup>б</sup>Факультет электроники и техники связи, группа учреждений КИЕТ

Газибад, Уттар-Прадеш (Индия) 201206

В этой работе оптоэлектронные, упругие и магнитные свойства  $\text{L}_{21}$  структурированных соединений Хейслера  $\text{Co}_2\text{VZ}$  ( $\text{Z} = \text{Pb, Si, Sn}$ ) были исследованы двумя методами. Одним из них является метод полнопотенциальной линейаризованной расширенной плоской волны (FP-LAPW), реализованный в WIEN2k, а вторым - метод псевдопотенциала, реализованный в Atomistic Tool Kit-Virtual NanoLab (ATK-VNL). Все эти соединения показывают нулевую ширину запрещенной зоны в основном канале спина в обоих кодах моделирования, и конечная запрещенная зона составляет 0,33 и 0,54 эВ в сплавах  $\text{Co}_2\text{VZ}$  ( $\text{Z} = \text{Pb, Sn}$ ) (полупроводниковых) соответственно. Причина в небольшом спиновом канале около уровня Ферми, что реализовано в коде WIEN2k со 100% спиновой поляризацией, за исключением  $\text{Co}_2\text{VSi}$  (металлик) с нулевой шириной запрещенной зоны. Эти соединения оказались идеально полуметаллическими ферромагнетиками (НМФ). Однако вышеупомянутые соединения показывают конечные запрещенные зоны в коде ATK-VNL. Рассчитанный магнитный момент этих соединений  $\text{Co}_2\text{VZ}$  ( $\text{Z} = \text{Pb, Si, Sn}$ ) составляет 3,00 и 3,00, 3,02 и 2,96, 3,00 и 3,00 мВ в кодах WIEN2k и ATK-VNL соответственно. Таким образом, мы наблюдали, что вычисленные значения по этим кодам моделирования и правилу Слейтера-Полинга имеют хорошо настраиваются. Были проанализированы оптические свойства этих соединений, такие как отражательная способность, показатель преломления, коэффициент возбуждения, коэффициент поглощения, оптическая проводимость и энергетические потери электронов. Коэффициент поглощения и значения функции энергетических потерь электронов увеличиваются по мере увеличения энергии. Соотношение  $\text{P}_{\text{в}}/\text{G}$  превышает 1,75 для всех соединений и показывает пластическую природу с положительным значением давления Коши ( $\text{CP} = \text{C}_{12} - \text{C}_{44}$ ) и показывает металлическое поведение соединений  $\text{Co}_2\text{VZ}$  ( $\text{Z} = \text{Pb, Si, Sn}$ ).

**КЛЮЧЕВЫЕ СЛОВА:** полуметаллический ферромагнетик, запрещенная зона, спинтроника, магнитный момент, упругие постоянные